

Advanced nanosphere lithography for the areal-density variation of periodic arrays of vertically aligned carbon nanofibers

Kyung Ho Park, Soonil Lee,^{a)} and Ken Ha Koh

Department of Molecular Science and Technology, Ajou University, Suwon 442-749, Korea

Rodrigo Lacerda, K. B. K. Teo, and W. I. Milne

Department of Engineering, University of Cambridge, Cambridge CB2 1PZ, United Kingdom

(Received 28 April 2004; accepted 12 October 2004; published online 27 December 2004)

Periodic arrays of vertically aligned isolated carbon nanofibers (CNFs) have been fabricated using self-assembled polystyrene spheres as shadow masks for catalyst-pattern formation. Proper use of monolayer and bilayer masks, and judicious combination of angle-deposition technique with monolayer masks have allowed us to control the dot size and spacing of catalyst patterns. As long as the catalyst-dot size is not too large, isolated single CNF has grown from each catalyst dot. Combining nanosphere lithography with conventional photolithography, we have been able to realize patterned growth of CNF arrays on selected areas. © 2005 The American Institute of Physics. [DOI: 10.1063/1.1829150]

I. INTRODUCTION

Vertically aligned carbon nanotubes have been studied vigorously due to their potential for applications in areas such as field-emission display, microwave amplifier, parallel electron-beam lithography, nanoelectronics, nanophotonics, and scanning probe microscopy.^{1–9} The synthesis of isolated carbon nanotubes and the concomitant control of their density are prerequisite to realizing the aforementioned applications. For example, geometrical field enhancement, which is the key to field-emission devices, depends strongly on the density of carbon nanotubes, and isolated single nanotubes are indispensable for scanning probe microscopy and nanoelectronics.^{7–9}

In general, plasma-enhanced chemical-vapor deposition (PECVD) methods are used to grow vertically aligned isolated carbon nanotubes with a high yield in a controllable manner. Since they are less crystalline and defect rich, these PECVD-grown carbon nanotubes are sometimes called, more fittingly, as carbon nanofibers (CNFs). It was reported previously that the catalyst-dot size should not exceed a certain limit to synthesize isolated single CNFs (ISCNFs); the dot size must be below 300 nm for the thickness of 7–10 nm.² To fabricate such small catalyst patterns, one of the expensive and difficult lithography techniques using e beam, focused ion beam, x ray, scanning tunneling microscopy, or atomic force microscopy has to be used.¹⁰ E-beam lithography, the most popular technique so far, is known for its excellent feature-size controllability, but its throughput is notoriously low and its cost is very high.

Recently, a method known as nanosphere lithography was proposed, as an alternative to e-beam lithography, for the pattern formation of periodic metal dots of nanometer size; nanospheres self-assembled onto substrates are used as shadow masks for metal deposition.^{11,12} Huang *et al.* applied

nanosphere lithography to the fabrication of catalyst patterns and demonstrated successful growth of ISCNFs.⁴ However, they used only small nanospheres (diameter $\leq 1 \mu\text{m}$) self-assembled into monolayers as shadow masks, and, therefore, their ISCNFs always formed hexagonal arrays with fixed spacing which, together with the CNF diameter, depended on the nanosphere size.

In this paper, we confirm that the diameter of vertically aligned CNFs and the spacing between themselves are scalable with the nanosphere size, and that the straightness of these CNFs, which are important for the photonic crystal application,⁵ are as good as their e-beam counterpart. Moreover, we report a few advanced nanosphere-lithography techniques, which allowed us to vary the pattern and spacing of catalyst dots, and, consequently, the density of vertically aligned CNFs.

II. EXPERIMENT

Commercially available (Duck Scientific Corp.) suspensions of monodisperse polystyrene spheres, diameter of 0.5, 1, and 2 μm , were used to form self-assembled shadow masks. Small amounts, 10–50 μL , of the suspensions were pipetted onto silicon substrates coated with 10-nm-thick SiO_2 or TiN diffusion-barrier layers. It is noteworthy that keeping the substrates tilted at about 6° during the self-assembly process was important to enlarge the domain sizes of the polystyrene spheres packed into ideal mono- and bilayer structures. After the deposition of 9-nm-thick Ni catalyst via evaporation or sputtering, the polystyrene-sphere masks were removed using toluene.

Vertically aligned CNFs were grown using the direct current PECVD. The feedstock was the mixture of acetylene and ammonia, and the growth temperature was about 630°C . The details of the CNF-growth conditions were presented elsewhere.¹³ The fabricated CNF arrays, together with the

^{a)}Author to whom correspondence should be addressed; electronic mail: soonil@ajou.ac.uk

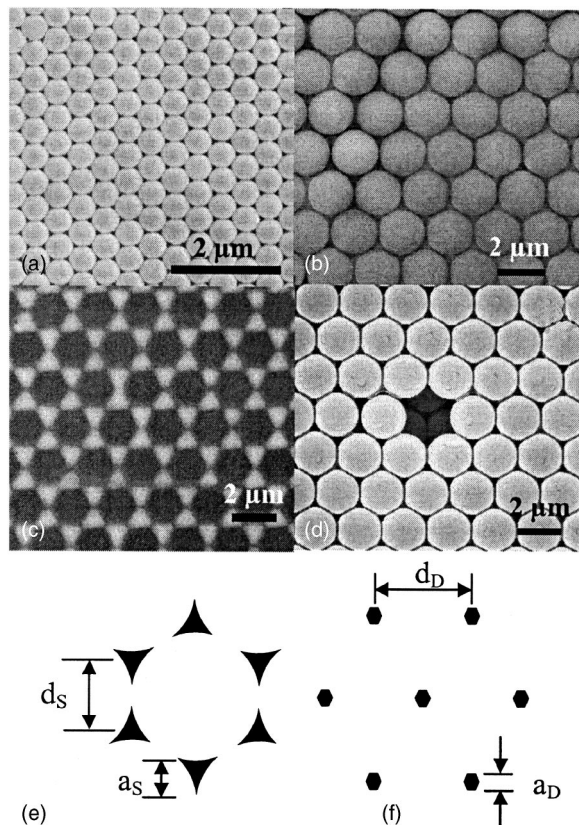


FIG. 1. SEM images of self-assembled monolayers of polystyrene spheres of (a) 0.5- and (b) 2- μm diameter, and catalyst dots formed using (c) monolayer and (d) bilayer of 2- μm spheres as shadow masks. Structural parameters, such as dot size and spacing, are marked in the schematic representation of the catalyst patterns corresponding to (e) monolayer- and (f) bilayer-shadow masks.

self-assembled-sphere masks and the catalyst-dot arrays, were examined using the scanning electron microscope (SEM), Hitachi S800 and S900.

III. RESULTS AND DISCUSSION

Figures 1(a) and 1(b) show typical SEM images of self-assembled monolayers of polystyrene spheres of 0.5- and 2- μm diameter, respectively. The polystyrene-sphere arrays function as shadow masks, and Ni catalyst can be deposited only through the interstices between three adjacent spheres to form hexagonal arrays of quasitriangular catalyst dots as presented in Fig. 1(c). However, in the case of self-assembled bilayer shown in Fig. 1(d), the interstices have different symmetries and, consequently, catalyst nanoparticles form a triangular array with a larger spacing. Figures 1(e) and 1(f) are schematic illustrations of catalyst nanoparticles formed using, respectively, mono- and bilayer shadow masks. Simple geometric calculation shows that the structural parameters of catalyst arrays, dot size (a_S and a_D) and spacing (d_S and d_D), depend on the sphere diameter D : $a_S = 0.232D$, $d_S = 0.577D$, $a_D = 0.155D$, and $d_D = D$.¹¹

Figure 2 shows a typical SEM image of ISCNF arrays grown on catalyst patterns formed using monolayer masks of 500-nm spheres. These ISCNF arrays have been fabricated using sputter-coated catalyst; however, it is found that there is no significant difference between sputtered and evaporated

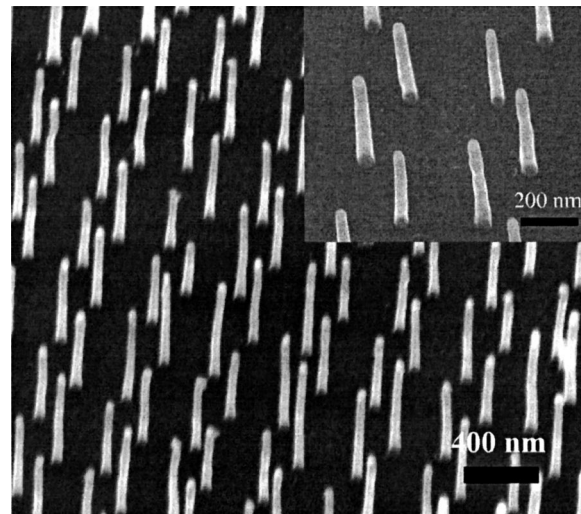


FIG. 2. A typical SEM image of ISCNF arrays grown on catalyst patterns formed using a monolayer mask of 500-nm spheres. The inset is the high-magnification image of the same ISCNF array.

catalysts. The high-magnification image in the inset clearly shows a hexagonal arrangement of vertically aligned ISCNFs. The diameter of CNFs and the spacing between CNFs are about 50 and 290 nm, respectively, and the straightness of CNFs is as good as that of CNFs grown on catalyst arrays formed using e-beam lithography.^{2,5} Similar ISCNF arrays (not shown here), but with larger CNF diameter and spacing of about 80 and 580 nm, are fabricated when 1- μm spheres are used to form self-assembled shadow masks. It is interesting to note that the diameters of these CNFs are very close to the isometric diameters, 51 and 81 nm, of 9-nm-thick catalyst nanodots of lateral sizes of 116 and 232 nm.^{2,13}

The factor-four difference in the CNF areal densities of these two arrays is the typical example of the automatic variation accompanying the selection of polystyrene-sphere size. However, as it turns out, the self-regulation of areal density of CNFs dependent on the polystyrene-sphere diameter is not sufficient to realize ISCNF arrays of density below $1.37 \times 10^8 \text{ cm}^{-2}$, which corresponds to the spacing of 750 nm. Note that when polystyrene spheres over 1.3- μm diameter are used to make the spacing larger than 750 nm, it is unavoidable for catalyst dots to exceed 300 nm, which is the aforementioned upper limit for the growth of ISCNFs.² The typical example of the multiple growth of CNFs from large catalyst dots is shown in Fig. 3(a); 1–4 CNFs grow from each catalyst dot when monolayer masks of 2- μm spheres are used.

The decrease of CNF density can be realized, without the multiple-growth problem, using larger polystyrene spheres self-assembled into bilayers [see Fig. 1(d)] as shadow masks for catalyst deposition. Compared with the monolayer masks formed using the same size spheres, the bilayer masks make the spacing between catalyst dots 1.73 times larger while reducing the dot size by 33%. Figure 3(b) shows the SEM image of ISCNF array fabricated using a bilayer mask of 2- μm spheres. Other than the halo, presumably corresponding to the residual catalyst at the edges of original catalyst dots, isolated single CNFs have grown from

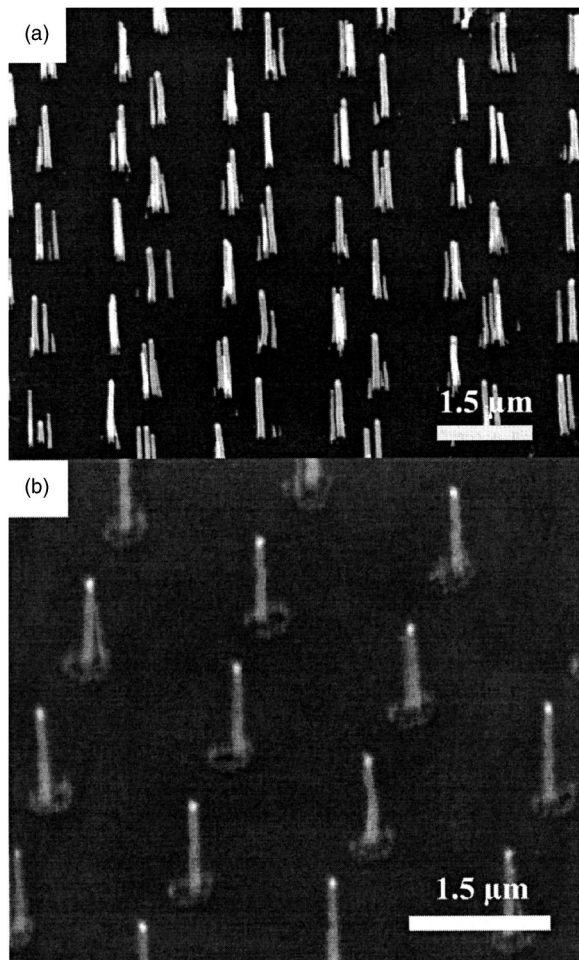


FIG. 3. SEM images of CNF arrays grown on catalyst patterns formed using (a) monolayer and (b) bilayer mask of 2- μm spheres. TiN and SiO₂ diffusion barrier has been used for (a) and (b), respectively.

each widely spaced catalyst dots. We attribute the halo effect to the combination of an inexplicably inhomogeneous adhesion of Ni catalyst to SiO₂ diffusion barrier and the peculiar concave shape of catalyst dots with trapezoidal cross section.¹¹ It is worth emphasizing that the halo effect is not observed if we use TiN diffusion barrier, or e-beam lithography is used, regardless of diffusion barrier, to form catalyst dots. An interesting feature of Fig. 3(b) is a slight distortion of the CNF-array pattern with respect to the original catalyst pattern. Note that each catalyst dot has conglomerated during the growth process without noticeable migration. However, the positions of the conglomerated catalysts do not coincide with the centers of the original catalyst dots.

The reduction of the catalyst-dot size for given catalyst patterns is an alternative way to lower CNF density without the multiple-growth problem. One way to reduce the effective size of catalyst is covering part of the catalyst with noncatalytic metals as shown in the inset of Fig. 4(a). The overlap of nanodots can be easily realized via the technique of angle deposition, which requires tilting of substrates relative to a deposition beam; the angle between the substrate normal and the deposition beam is defined as the deposition angle θ_{dep} . The overlap of quasitriangular Ni and Cr dots shown in the inset of Fig. 4(a) have been produced by depositing Ni

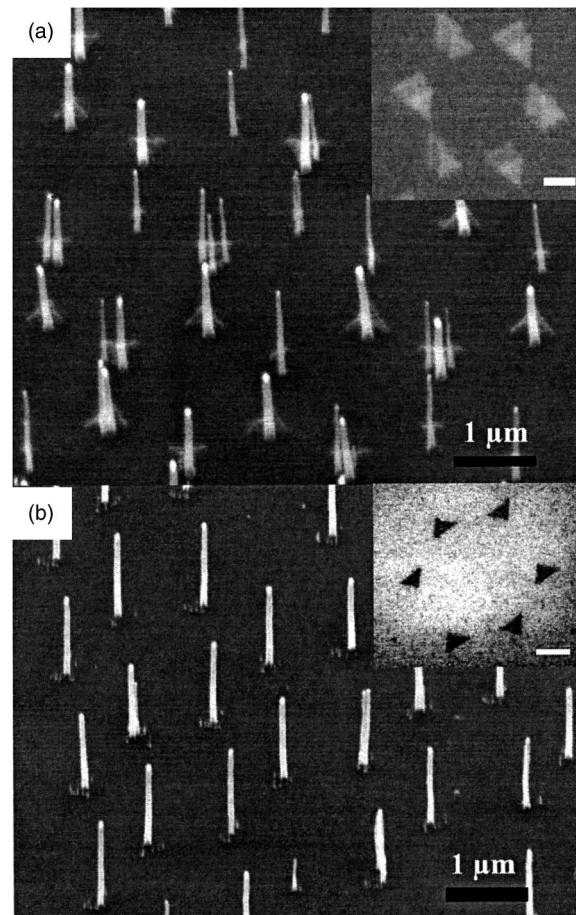


FIG. 4. SEM images of CNF arrays grown on catalyst patterns formed via the deposition of (a) Ni and Cr at different deposition angles, $\theta_{\text{dep}}=0^\circ$ and $\theta_{\text{dep}}=15^\circ$, in succession, and (b) Ni at a high deposition angle ($\theta_{\text{dep}}=30^\circ$) using monolayer masks of 2- μm spheres. The insets show the catalyst dots; the scale bar corresponds to 600 nm.

and Cr at $\theta_{\text{dep}}=0^\circ$ and $\theta_{\text{dep}}=15^\circ$ in succession using the monolayer mask of 2- μm spheres. Compared with Fig. 3(a), we find that the multiple-growth problem is significantly subdued in the CNF arrays fabricated using this catalyst pattern of overlap structure; see Fig. 4(a). As a variation of the overlap method, reversing the order of the deposition sequence of catalyst and noncatalytic materials has worked as well. In this case, we have realized the reduction of catalyst dot via the lift-off process using noncatalytic material as a sacrificial layer. Note that the overlap procedure can be improved to make smaller catalyst dots, which is necessary for the complete suppression of multiple growth, by rotating substrates during the deposition of noncatalytic materials.

Another way to reduce the size of catalyst for the given shadow mask of self-assembled spheres is by using a high deposition angle. As shown in the inset of Fig. 4(b), the deposition at $\theta_{\text{dep}}=30^\circ$ using the monolayer mask of 2- μm spheres has resulted in substantial reduction of catalyst size while maintaining the hexagonal catalyst pattern. Moreover, Fig. 4(b) shows the growth of vertically aligned ISCNFs from these high-angle-deposited catalyst dots. We expect that the diameter control of CNFs, while maintaining the overall pattern shape, will be possible through the adjustment of the deposition angle with the self-assembled masks of identical sphere size.

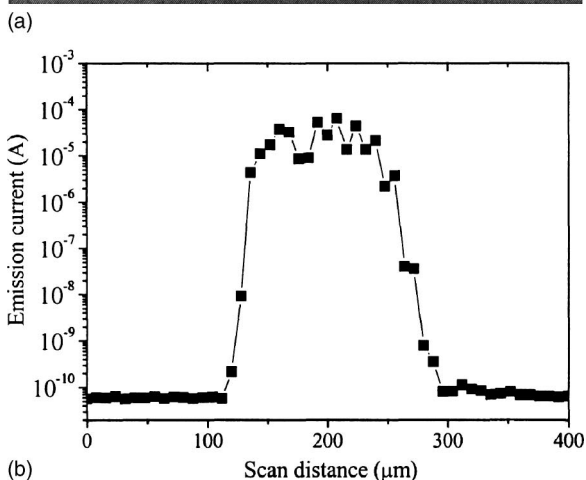
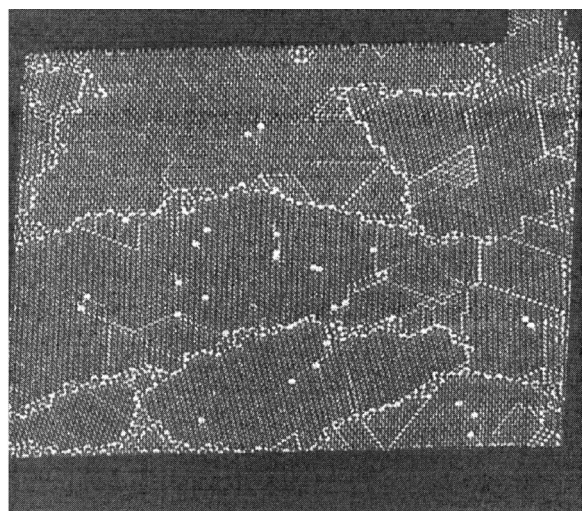


FIG. 5. (a) Low-magnification SEM image of a $180 \times 180\text{-}\mu\text{m}^2$ square which consists of vertically aligned CNF array fabricated using a $2\text{-}\mu\text{m}$ sphere mask and (b) the line scan of its field-emission currents measured at constant-field mode using a tungsten-tip anode.

It is noteworthy that nanosphere lithography can be combined with conventional photolithography for the patterning and area-selective fabrication of CNF arrays. Photoresist layers, the thickness of which is similar with that of either the monolayer or bilayer of polystyrene spheres, have been patterned and filled with suspensions of monodisperse polystyrene spheres to form self-assembled shadow masks only in selected areas. After the deposition of catalyst, the photoresist has been lifted off. Figure 5(a) shows low-magnification SEM image of a $180 \times 180\text{-}\mu\text{m}^2$ square which consists of vertically aligned CNF array fabricated using $2\text{-}\mu\text{m}$ spheres mask. The defects in Fig. 5(a) reflect grain boundary and vacancies in the polystyrene-sphere array, through which

larger catalysts and consequently multiple CNFs have been formed. Presumably, the size mismatch between the polystyrene-sphere array and photoresist pattern and the surface change after the photolithography process are responsible for the grain boundary and vacancies, respectively. We are confident that these defects can be removed with a better control of the photolithography process. The line-scan result in Fig. 5(b) is the field-emission currents measured at the constant voltage of 1400 V and the gap of $18\text{ }\mu\text{m}$, respectively, using an $\sim 17\text{-}\mu\text{m}$ tungsten-tip anode in $8\text{-}\mu\text{m}$ steps. This linear-scan result shows that only CNFs in the square area of $180 \times 180\text{ }\mu\text{m}^2$ contribute emission currents, and that there are no CNFs at all outside of this square area.

IV. CONCLUSION

In conclusion, we have successfully fabricated vertically aligned ISCNF arrays on catalyst patterns formed using self-assembled polystyrene spheres as shadow masks. Moreover, we have been able to overcome the CNF-density lower limit imposed by the geometry of the monolayer masks using the bilayer masks, the successive deposition of catalyst and non-catalyst at different deposition angles, or the high deposition angle. Finally, we have demonstrated that nanosphere lithography can be combined with conventional photolithography to generate desired patterns made of vertically aligned CNF arrays.

ACKNOWLEDGMENTS

This work was supported by the postdoctoral fellowship program of Korea Science and Engineering Foundation. One of the authors (S. L.) acknowledges support from the ABRL Program of KOSEF through Grant No. R14-2002-062-01000-0.

- ¹Z. F. Ren *et al.*, *Appl. Phys. Lett.* **75**, 1086 (1999).
- ²K. B. K. Teo *et al.*, *Nanotechnology* **14**, 204 (2003).
- ³V. I. Merkulov, D. H. Lowndes, Y. Y. Wei, G. Eres, and E. Voelkl, *Appl. Phys. Lett.* **76**, 3555 (2000).
- ⁴Z. P. Huang *et al.*, *Appl. Phys. Lett.* **82**, 460 (2003).
- ⁵K. Kempa *et al.*, *Nano Lett.* **3**, 13 (2003).
- ⁶K. B. K. Teo *et al.*, *J. Vac. Sci. Technol. B* **21**, 693 (2003).
- ⁷S. H. Jo, Y. Tu, Z. P. Huang, D. L. Carnahan, D. Z. Wang, and Z. F. Ren, *Appl. Phys. Lett.* **82**, 3520 (2003).
- ⁸M. A. Lantz, B. Gotsmann, U. T. Dürig, P. Vettiger, Y. Nakayama, T. Shimizu, and H. Tokumoto, *Appl. Phys. Lett.* **83**, 1266 (2003).
- ⁹X. Yang *et al.*, *Nano Lett.* **3**, 1751 (2003).
- ¹⁰Y. Xia, J. A. Rogers, K. E. Paul, and G. H. Whitesides, *Chem. Rev.* (Washington, D.C.) **99**, 1823 (1999).
- ¹¹J. C. Hulteen, D. A. Trechel, M. T. Smith, M. L. Duval, T. R. Jensen, and R. P. Van Duyne, *J. Phys. Chem.* **103**, 3854 (1999).
- ¹²C. L. Haynes, A. D. McFarland, M. T. Smith, J. C. Hulteen, and R. P. Van Duyne, *J. Phys. Chem.* **106**, 1898 (2002).
- ¹³M. Chhowalla *et al.*, *J. Appl. Phys.* **90**, 5308 (2001).